

Article

# A New Approach for Modeling Vertical Dynamics of Motorcycles Based on Graph Theory

Mouad Garziad <sup>1,\*</sup>, Abdelmjid Saka <sup>2</sup>, Hassane Moustabchir <sup>2</sup> and Maria Luminita Scutaru <sup>3,\*</sup>

<sup>1</sup> Mechanical Engineering Laboratory, Faculty of Science and Technology, Sidi Mohamed Ben Abdellah University, B.P. 2202 Route d'Imouzzer, Fez 30000, Morocco

<sup>2</sup> Laboratory of Science Engineering and Applications, National School of Applied Sciences, Sidi Mohamed Ben Abdellah University, BP 72 Route d'Imouzzer, Fez 30000, Morocco; abdelmjid.saka@usmba.ac.ma (A.S.); hassan.moustabchir@usmba.ac.ma (H.M.)

<sup>3</sup> Department of Mechanical Engineering, Transilvania University of Braşov, 500036 Braşov, Romania

\* Correspondence: mouad.garziad@usmba.ac.ma (M.G.); lscutaru@unitbv.ro (M.L.S.)

**Abstract:** The main objective of this research is to establish a new formulation and mathematical model based on graph theory to create dynamic equations and provide clarity on the fundamental formulation. We have employed graph theory as a new approach to develop a new representation and formulate the vertical dynamics of a motorcycle with four degrees of freedom, including a suspension and tire model. We have outlined the principal procedural steps required to generate the mathematical and dynamic equations. This systematic approach ensures clarity and precision in our formulation process and representation. Subsequently, we implemented the dynamics equations to examine the dynamic behavior of both the sprung and unsprung masses' vertical displacements, while considering the varying conditions of the road profile.

**Keywords:** motorcycle dynamics; vertical dynamics; symbolic computing; simulation; graph theory; tire; suspension

**MSC:** 70G60



**Citation:** Garziad, M.; Saka, A.; Moustabchir, H.; Scutaru, M.L. A New Approach for Modeling Vertical Dynamics of Motorcycles Based on Graph Theory. *Mathematics* **2024**, *12*, 1390. <https://doi.org/10.3390/math12091390>

Received: 6 March 2024

Revised: 27 April 2024

Accepted: 28 April 2024

Published: 2 May 2024



**Copyright:** © 2024 by the authors. Licensee MDPI, Basel, Switzerland. This article is an open access article distributed under the terms and conditions of the Creative Commons Attribution (CC BY) license (<https://creativecommons.org/licenses/by/4.0/>).

## 1. Introduction

Graph theory is the study of mathematical structures called graphs [1]. These graphs model the relationships between objects, with nodes representing the objects, and edges representing the pairwise connections between them. Since the early 1960s, research in the area of vehicle dynamics has gradually become more systematic and intensive. Indeed, mathematical modeling has become an important step in understanding the dynamics of the system. During the formulation stage, two methods can generate system equations: symbolic and numerical approaches. The numerical approach involves representing the system using matrices at a specific time. The symbolic approach generates mathematical expressions that describe the system for all time [2]. In conventional modeling methods, equations are manually derived. In contrast, graph theory allows for automatic generation of governing equations. Graph-theoretic modeling (GTM) is a practical approach for kinematic and dynamic analysis of multibody systems [3]. The main purpose of this article is to establish a new formulation and model for a motorcycle in a graph-theoretical context. Importantly, a steady increase in modeling and formulation has resulted in the self-formulation and automatic generation of the governing equation of motion for any mechanical system. A few symbolic formulation techniques have been developed in recent years to represent vehicle systems using graph theory concepts. However, tires are one of the most significant components of vehicles that are treated and analyzed by using graph theory. The aim of this research is to develop formulations that automatically derive the equations of motion for a half-vehicle system utilizing graph-theoretic modeling. In

this paper, we introduce a multi-terminal component model for analyzing the kinematics and dynamics of the motorcycle model. Consequently, our paper examines the modeling dynamics of a motorcycle in a vertical position and with a pitch rotation angle using graph-theoretic modeling (GTM). Numerous researchers have focused on modeling mathematical equations for motorcycles. Those working in this field, which concerns vehicle dynamics, confirm that this model is crucial for studying a vehicle's dynamic behavior. Garziad and Saka [4] provided an overview of the use and applications of graph theory concepts in modeling. And the analysis of systems in various fields, such as vehicle dynamics, has led to the development of novel techniques aimed at enhancing computational efficiency and analysis. Bombardier and colleagues [5] developed a novel method that employs a linear graph to depict the tire–road interaction. They also utilized a symbolic approach to formulating governing equations. Similarly, in their research, Schmitke et al. [6] utilized graph theory and the principle of orthogonality to compute tire forces and moments. They incorporated a tire model into a symbolic computer program that generates real-time simulations of vehicle dynamics. The tire component of the program produces symbolic expressions for important variables such as inclination and slip angle. In their analysis of the torque converter of an automotive vehicle, Banerjee and McPhee [7] employed a linear graph to model its behavior. They aimed to develop a governing equation for the torque converter in symbolic form and compared it with conventional modeling methods by simulating the system of equations in a symbolic environment. Belkaloul [8] worked on designing a model of a vehicle with a trailer. He used the vector network method and the concept of a multibody system to make a three-dimensional model of the trailer with six degrees of freedom. Additionally, he developed differential equations to accurately describe the movement of the vehicle. Schmitke and McPhee [9] invented the symbolic formulation method, which uses linear graph theory and orthogonality principles to generate governing equations for vehicle systems. This method was further developed into a package called DynaFlexPro, which includes a tire component called DynaFlexPro/Tire that can be used to simulate vehicle dynamics. The study conducted by Al-Hakim et al. [10] used graph theory to demonstrate the connections between the parts of a product. They applied graph theory concepts to depict the energy flow and utilized it to design various components such as sliding gears, clutches, overrunning clutches, and flywheels. In their paper, Vogt et al. [11] introduced a detailed electric vehicle model utilizing graph-theoretic modeling. The model was constructed with the aid of Maple/DynaFlexPro's BuildEQs version 2.3, which facilitated the streamlining and formulation of the electric vehicle's governing equations.

Several studies have showcased the integration of graph theory into diverse engineering applications, enhancing analytical methods and computational modeling techniques. Dunlop and Khajepour [12] utilized graph theory to develop dynamic equations for a drive belt pulley mechanism, employing a hybrid branch–chord approach. Sreeram [13] introduced a novel method for analyzing parametric design in torsional vibrating systems, utilizing directed graphs to model system characteristics and predicting parametric values' direction of change. Redmond and McPhee [14] automated the formulation of multibody kinematic and dynamic equations using indirect coordinates, introducing virtual joints between bodies within a graph-theoretical framework. Schmitke et al. [15] integrated graph theory and the principle of orthogonality to compute tire forces and moments, employing symbolic formulation based on linear graph theory for vehicle dynamics simulations, thereby enhancing computational efficiency and accuracy.

So, based on the previous studies, mainly in mechanical modelling, graph theory deals with static relationships among entities rather than dynamic behaviors. Although it can be utilized to depict the connections and interactions among rigid bodies within multibody systems, it might lack the necessary tools for thorough dynamic analysis, including precise calculations of forces, accelerations, and velocities.

This paper is organized as follows. The first part is a literature review of the vehicle field in which the graph theory concept is used. The second part illustrates how graph theory is

utilized to ensure the self-formulation of the governing equations. Then, the third part discusses in detail the steps to produce and generate the dynamic equations of a system.

## 2. Graph Theory Formulation

### 2.1. Method Overview

To generate mechanical and dynamic equations using graph theory, one must represent the mechanical system as a graph and then derive equations based on the properties and connections of the graph. Here are the steps to generate the governing equations for a system [16,17]:

- To begin, identify the various components of your mechanical system. These may include masses, springs, dampers, rigid bodies, and other relevant elements. Once identified, assign nodes to each component within the graph.
- For each component of the system, create a node. These nodes may represent masses, joints, or other key points. Physical connections between nodes, such as springs or dampers, are represented by edges. The type of connection will determine the edge's properties.
- Assign properties to the edges that represent physical connections between components. For springs, the edge may have a spring constant ( $k$ ), while for dampers, it could have a damping coefficient ( $c$ ). These properties will be used to derive equations later.
- Define a suitable coordinate system for the mechanical system. This involves selecting reference points and directions for displacement and forces. This step is crucial as it determines how the equations will be expressed.
- Assign variables to represent the displacements of nodes in the chosen coordinate system. These variables are typically functions of time (e.g.,  $x(t)$ ,  $y(t)$ ,  $z(t)$ ).
- For each node, apply Newton's second law to write down the equations of motion based on the forces acting on the node. These forces can include applied forces, spring forces, and damping forces. Express these forces in terms of the node displacements and any known properties.
- Set the equations of motion to zero to find equilibrium positions. Combine the equations of motion from each node to form a system of differential equations. This system of equations will describe the dynamic behavior of the mechanical system.
- Solve these equations analytically or numerically.
- Implement the equations to study the dynamic behavior of your mechanical system.

### 2.2. Representation and Conception of Graph

Graph-theoretic modeling (GTM) is a valuable method for analyzing and modeling entire systems. This technique uses graph theory to represent physical systems as a group of nodes and edges. In mechanical systems, nodes indicate reference frames, while edges represent transformations between these reference frames. Furthermore, a linear graph's edge has two variable types: across variables, which are quantities measured in parallel with the edge by a device, and through variables [18–20], which are quantities measured in series with the edge by a device. In the mechanical translational domain, through variables are forces  $\bar{F}$  and across variables are positions  $\bar{r}$ , velocities  $\bar{v}$ , and accelerations  $\bar{a}$ . In the mechanical rotational domain, through variables are moments  $\bar{M}$  and across variables are angles  $\bar{\theta}$ , angular velocities  $\bar{\omega}$ , and angular accelerations  $\bar{\alpha}$ .

To derive the governing equations of motion, formulation techniques are used to link the component equations of systems with their topological equations, which are obtained from the system graph. Several methods exist to create the system graph and obtain the related topological equations, and these techniques have been cited in [21–23].

## 3. Physical Modeling of Vertical Dynamics of Motorcycles

### 3.1. System Description

The physical modeling of the vertical dynamics of a motorcycle involves describing and simulating the motion of the motorcycle and its components in response to various forces and inputs. Studying vertical dynamics involves analyzing how a vehicle responds

to vibrations and forces. This is important in designing a suspension system as it affects a car’s stability and control. When examining the vertical dynamics of a motorcycle, three crucial components are considered. These components include:

- Sprung mass ( $m_s$ ): the weight of all the components of the car that rest on the suspension system (such as the chassis, engine, and transmission).
- Unsprung mass ( $m_u$ ): the weight of all the components located in the wheel hub, such as the hub itself, brake disk and caliper, axle, tire, wheel rim, etc.
- The suspension system comprises various components that connect the sprung mass to the unsprung mass. It plays a crucial role in ensuring both comfort and handling while driving.

The proposed motorcycle model is displayed in Figure 1 below:

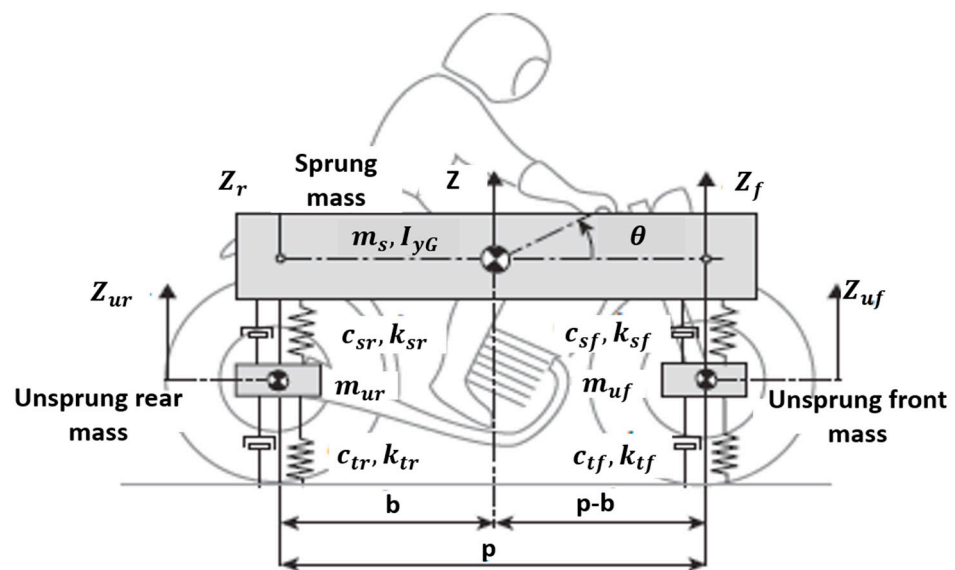


Figure 1. Motorcycle model (reproduced from V. Cossalter [24]).

The components of a motorcycle in a vertical position are summarized in Table 1 below, which outlines the relevant parameters.

Table 1. Notation.

Parameter	Nomenclature
Sprung Mass	$m_s$
Moment of inertia of the motorcycle body	$I_{yG}$
Front unsprung mass	$m_{uf}$
Rear unsprung mass	$m_{ur}$
Wheelbase	$p$
Rear wheelbase	$b$
Rear and front suspension stiffness	$k_{rs}, k_{fs}$
Front and rear tire stiffness	$k_{if}, k_{tr}$
Front and rear suspension damping coefficient	$C_f, C_r$
Rear and front tire damping coefficient	$C_{tr}, C_{if}$
Pitch angle	$\theta$
Rear and front vertical coordinate	$z_r, z_f$
Rear and front vertical coordinate of unsprung mass	$z_{ur}, z_{uf}$

The numerical values and parameters utilized in our model are specified in Appendix A, Table A1.

### 3.2. Hypotheses

In the modeling process and development of a new approach, the hypotheses play a crucial role in mathematical development by providing a structured framework for conceptualizing, constructing, and evaluating models of complex systems.

The modeling of the vertical dynamics of a motorcycle involves considering various factors such as the mass distribution, suspension characteristics, tire properties, and external forces acting on the system.

The hypotheses behind our motorcycle model are as follows:

- The moment caused by weight overturning  $-m.g.d_{roll}$  has been ignored; no assumptions have been made regarding the height of the pitch center in relation to the ground.
- The vertical dynamics of a motorcycle tire can be effectively modeled as a rigid body under certain conditions.
- Tire deformations are negligible compared to its dimensions, and the tire maintains contact with the ground.
- Tires are commonly known to be rigid, lacking flexibility. As a result, they do not provide much compliance.
- It is assumed that the longitudinal positions of both the springs and the shock absorber are identical.
- There are no aerodynamic forces being taken into consideration.
- The stiffness and damping values pertain to the entire axle and are attributed to a singular spring or shock absorber.
- The mass and moment of inertia are referring to the whole weight of the vehicle's suspension system.
- The vehicle's body is considered to be a rigid body.

## 4. Linear Graph Representation

### 4.1. Graph Representation of the System

The front and rear suspension systems of a motorcycle are responsible for supporting the weight of the vehicle. These systems are designed with specific stiffness and damping characteristics. The front suspension is attached to the front unsprung mass, while the rear suspension is attached to the rear unsprung mass. When analyzing the motorcycle theoretically, it is often treated as a rigid body, with the sprung mass acting like a simply supported rigid beam. While there may be interactions between the body structure and wheels, this simplification allows for easier analysis.

Below is the graph equivalent of the system:

The Figure 2 represent the graphical representation of motorcycle. The graph above depicts node  $Q$ , which represents the ground's fixed frame of reference. The graph's edges represent the system's components, while the nodes  $A$ ,  $B$ ,  $C$ ,  $D$ , and  $E$  indicate physical connection points. Therefore, the system's motion relative to an inertial frame (at node  $Q$ ) can be observed. The mass of the rear and front tire is represented by edges  $M_1$ ,  $M_2$ ; the edge  $M_3$  represents the mass and the rotational inertia of the mainframe; the rigid arm element is denoted by  $T_{11}$ ;  $T_{12}$  corresponds to the position vector that locates the rigid body positions on the ground;  $F_p$  is the weight of the vehicle body; the edges  $K_3$  and  $K_4$  represent the suspension of the system; the edges  $K_1$ ,  $K_2$  represent the tire; and  $N_1$ ,  $N_2$  represent the reaction force. These variables are used to represent the system.

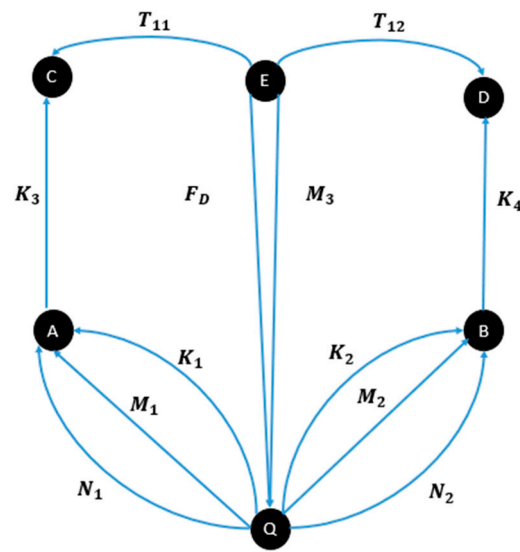


Figure 2. A graphical representation of the motorcycle.

A summary of these graph edges is given in Table 2:

Table 2. Terminal equations for tire–road model.

Edge	Description
$M_1, M_2$	Masses of front and rear tire
$M_3$	Rotational inertia
$T_{11}, T_{12}$	Rigid arm (define centroidal position on a mass)
$K_3, K_4$	Rear and front suspension element
$K_1, K_2$	Front and rear elastic tire
$N_1, N_2$	Front and rear reaction force
$F_D$	Weight force

#### 4.2. Constitutive Equations

For system modeling, a set of topological equations is essential to accurately describe the interconnections and relationships between various components or elements within the system. These equations define the topology of the system, representing its structure and configuration in mathematical terms. They outline the connectivity between different nodes or elements, as well as the flow of information, energy, or other relevant quantities throughout the system.

##### Rigid body element

###### - The inertial element

The edge  $M_3$  describes the specific characteristics and properties associated with the inertia of the mainframe. These equations may include parameters such as the mass, moments of inertia, and distribution of mass within the motorcycle body. Additionally, they might encompass terms related to the rotational or translational motion of the mainframe, depending on the system’s configuration and requirements.

The terminal equation for this edge is

$$\bar{T}_{M3} = -I\bar{\alpha} - \bar{r}_{T11} \times \bar{F}_{T11} \tag{1}$$

where  $I$  represents the moments of inertia;  $-\bar{r}_{T11} \times \bar{F}_{T11}$  represents the torque generated by the force  $\bar{F}_{T11}$ , applied at point  $T_{11}$  on the rigid body; and  $-\bar{r}_{T11}$  is the position vector from the axis of rotation to point  $T_{11}$ .

- **The mass elements**

The edges  $M_1, M_2,$  and  $M_3$  symbolize the masses of critical components within the system: the rear tire, front tire, and mainframe, respectively. Each of these components contributes significantly to the overall dynamics and performance of the system, with their masses influencing factors such as acceleration, maneuverability, and stability.

The terminal equations for these edges represent the specific characteristics and properties associated with each component’s mass. For the rear tire (edge  $M_1$ ) and front tire (edge  $M_2$ ), the terminal equations might include parameters such as the tire mass, rotational inertia, and distribution of mass around the tire’s axis.

Similarly, the terminal equations for the mainframe (edge  $M_3$ ) describe its mass distribution and moments of inertia.

The terminal equation for these edges is

$$\bar{T}_M = -m.\ddot{\bar{r}} \tag{2}$$

where  $\bar{r} = \begin{pmatrix} 0 \\ 0 \\ \bar{z} \end{pmatrix}$  represents the translational across variable.

**The rigid arm element**

The  $T_{11}$  and  $T_{12}$  edges represent the rigid arm element, denoting the geometric transformation from the mainframe’s center of mass to a point on the body fixed to a frame. As previously explained, the terminal equations that describe the behavior of the rigid arm element at the end of its motion are provided. For the translational domain, the terminal equations for the system’s equations can be expressed as follows:

$$\begin{aligned} \bar{F}_r &= \begin{Bmatrix} \bar{F}_r \\ \bar{F}_r \end{Bmatrix} \\ \bar{r}_{T110} &= \begin{Bmatrix} a \\ 0 \end{Bmatrix} \\ \bar{r}_{T120} &= \begin{Bmatrix} b \\ 0 \end{Bmatrix} \end{aligned} \tag{3}$$

and the symbolic variables describe the translational through variable  $\bar{F}_r$  for the edge representing the rigid arm element as vectors.

Equation (4) represents the acceleration of a point  $\bar{r}_r$  relative to a reference frame.

$$\begin{aligned} \bar{r}_{T11} &= R_{M3}.\bar{r}_{T110} \\ \bar{r}_{T12} &= R_{M3}.\bar{r}_{T120} \\ \dot{\bar{r}}_r &= \bar{v}_r = \bar{\omega}_M \times r_r \\ \ddot{\bar{r}}_r &= \bar{a}_r = \dot{\bar{r}}_r = \dot{\bar{\omega}}_r.\bar{r}_r - (\bar{\omega}_M)^2 \times \bar{r}_r \end{aligned} \tag{4}$$

**Tire element**

The edges  $K_1, K_2$  represent the tire element. This element is characterized just by vertical displacement. In fact, it takes into account the elastic behavior of the tire. The terminal equation for these edges is

$$\bar{T}_k = -K_{tire}(\bar{r}_r - \bar{r}_{road}) \tag{5}$$

$r_{road}$  represents the position of the road, and  $(\bar{r}_r - \bar{r}_{road})$  represents the relative displacement between the tire’s contact point and the corresponding point on the road surface.

### Suspension element

The edges  $K_3, K_4$  represent the suspension of the vehicle body that connect the main-frame with the tire using a damper and spring. The terminal equation for these edges is

$$\bar{T}_K = \left( -K(\bar{r}_r - \bar{r}_0) - d\dot{\bar{r}}_r \cdot \bar{u} \right) \cdot \bar{u} \tag{6}$$

$\bar{r}_r - \bar{r}_0$  represents the displacement of the system from its reference position, and  $d\dot{\bar{r}}_r \cdot \bar{u}$  represents the force exerted by damping, where  $d$  is the damping constant.

### The external force element

The edge  $\bar{T}_{Fp}$  represents the force exerted on the mainframe due to its mass, which is called the body force. In graph theory, this is called a through vertex and is associated with terminal equations:

- For the translational domain:

$$\bar{T}_{FD} = \begin{Bmatrix} -m \cdot \bar{g} \\ 0 \end{Bmatrix} \tag{7}$$

- For the rotational domain:

$$\bar{\tau}_{FD} = \{0\}^{3 \times 3} \tag{8}$$

$\bar{\tau}_{Fp}$  represents the torque vector, and  $\{0\}^{3 \times 3}$  represents a  $3 \times 3$  matrix filled with zero vectors.

### Rotation matrix element

The rotation matrix serves as a fundamental mathematical tool for representing and manipulating rotations in 2D and 3D space. It enables the transformation of vectors and coordinates between different coordinate systems or frames of reference, facilitating geometric calculations and analysis. The rotation matrix can be defined as

$$R_M = \begin{pmatrix} \cos \theta & -\sin \theta \\ \sin \theta & \cos \theta \end{pmatrix} \tag{9}$$

The terminal equations are summarized in Table 3.

**Table 3.** Terminal Equations.

Component	Terminal Equations
$\bar{F}_{M1}, \bar{F}_{M2}, \bar{F}_{M3}$	$\bar{F} = -m \cdot \frac{\partial}{\partial t}(\bar{r}), \bar{r} = \begin{pmatrix} 0 \\ 0 \\ \bar{z} \end{pmatrix}$
$\bar{T}_{M3}$	$\bar{T} = -I \cdot \bar{\alpha} - \bar{\omega} \times (I \cdot \bar{\omega})$
$\bar{F}_{T11}, \bar{F}_{T12}$	$\begin{aligned} \bar{r}_r &= R_M \cdot \bar{r}_0 \\ \dot{\bar{r}}_r &= \bar{\omega}_M \times \bar{r}_0 \\ \ddot{\bar{r}}_r &= \dot{\bar{\omega}}_M \cdot \bar{r}_0 - (\bar{\omega}_M)^2 \times \bar{r}_0 \\ R_M &= \begin{pmatrix} \cos \theta & -\sin \theta \\ \sin \theta & \cos \theta \end{pmatrix} \end{aligned}$
$\bar{F}_{K3}, \bar{F}_{K4}$	$\bar{F} = \left( -K(\bar{r}_r - \bar{r}_0) - d\dot{\bar{r}}_r \cdot \bar{u} \right) \cdot \bar{u}$
$\bar{F}_{K1}, \bar{F}_{K2}$	$\bar{F} = -K_{tire}(\bar{r}_r - \bar{r}_{road})$
$\bar{N}_F, \bar{N}_R, \bar{F}_P,$	$\begin{aligned} \dot{\bar{T}} &= \dot{\bar{T}}(t) \\ \bar{F} &= \bar{F}(t) \\ \bar{F} &= -m \cdot \bar{g} \end{aligned}$

### 5. Motion Equations

#### 5.1. Equation of Dynamics

We can create a group of equations by utilizing rotational and translational cutset equations in conjunction with terminal equations [25,26]. To obtain the system’s equations of motion, we project the rotational tree elements onto the system’s coordinates. These cutset equations establish the connections between the through variables, derived from the system graph.

The equations for the projected translational cutset result in this system serve as a critical component in the analysis and understanding of the system’s translational dynamics. These equations capture the relationships between various forces, velocities, and accelerations acting on the system, providing valuable insights into its motion.

The equations for the projected translational cutset result in this system are

$$\begin{aligned} [\bar{F}_{T11} + \bar{F}_{T12} + \bar{F}_{K4} + \bar{F}_{K3} + \bar{F}_P + \bar{F}_{M3}] \cdot \{\hat{u}_z\} &= \bar{0} \\ [\bar{F}_{M1} + \bar{F}_{N1} + \bar{F}_{K1} + \bar{F}_{K3}] \cdot \{\hat{u}_z\} &= \bar{0} \\ [\bar{F}_{M1} + \bar{F}_{N1} + \bar{F}_{K1} + \bar{F}_{K3}] \cdot \{\hat{u}_z\} &= \bar{0} \\ [\bar{F}_{M1} + \bar{F}_{K1} + \bar{F}_{N1} + \bar{F}_{M2} + \bar{F}_{K2} + \bar{F}_P + \bar{F}_{M3}] \cdot \{\hat{u}_z\} &= \bar{0} \end{aligned} \tag{10}$$

By substituting the terminal equations, we can obtain the following set of equations:

$$\begin{aligned} \bar{F}_{M1} + \bar{F}_{N1} + \bar{F}_{K1} + \bar{F}_{K3} &= \bar{0} \\ -m \cdot \ddot{\bar{z}}_{ur} + \bar{N}_r - k_{ft}(\bar{r}_{TA} - \bar{r}_{TQ}) + \bar{F}_{K3} &= \bar{0} \end{aligned} \tag{11}$$

with

$$\begin{aligned} \bar{F}_{M2} + \bar{F}_{K2} + \bar{F}_{K2} + \bar{F}_{N2} + \bar{F}_{K4} &= \bar{0} \\ -m \cdot \ddot{\bar{z}}_{uf} + \bar{N}_f - k_{ft}(\bar{r}_{TB} - \bar{r}_{TQ}) + \bar{F}_{K4} &= \bar{0} \end{aligned} \tag{12}$$

By substituting the terminal equations into the relevant expressions, we can derive a set of equations that describe the system’s behavior based on the relationships established by the terminal equations.

$$\begin{aligned} \bar{F}_{K4} &= (k_{sf}(\bar{r}_D - \bar{r}_B) + (C_{sf} \cdot \dot{\bar{r}}_{TD})) \\ \bar{F}_{M3} + \bar{F}_{T11} + \bar{F}_{T12} + \bar{F}_{K4} + \bar{F}_{K3} + \bar{F}_P &= \bar{0} \\ -m \cdot \ddot{\bar{z}}_s - m \cdot \bar{g} - (k_{sf}(\bar{r}_D - \bar{r}_B) + (C_{sf} \cdot \dot{\bar{r}}_{TD})) - (k_{sf}(\bar{r}_A - \bar{r}_{TQ}) + (C_{sf} \cdot \dot{\bar{r}}_{TA})) &= \bar{0} \end{aligned} \tag{13}$$

- **Rotational cutset equations**

To analyze the rotational characteristic, we can project the cutset equations onto the motion space that represents the mainframe’s rotation axis [18]. In this case, the motion space is the k-axis, and the cutset equations are described below:

$$[\bar{T}_{M3} + \bar{T}_{T12} + \bar{T}_{T11} + \bar{T}_{Fp} + \bar{T}_{K3} + \bar{T}_{K4}] \cdot \{\hat{k}\} = \bar{0} \tag{14}$$

and by substituting the terminal equations, the equivalent equations are

$$-I \cdot \bar{\alpha} - \bar{r}_{T11} \times \bar{F}_{T11} - \bar{r}_{T12} \times \bar{F}_{T12} = \bar{0} \tag{15}$$

or

$$\begin{aligned} \bar{r}_{T11} &= R_m \cdot \bar{r}_{T110} \\ \bar{r}_{T12} &= R_m \cdot \bar{r}_{T120} \end{aligned} \tag{16}$$

By substituting the transformation equations into the relevant expressions, we can derive a new set of equations that describe the system’s behavior based on the transformed variables. These transformation equations provide a means of converting between different coordinate systems or representations, allowing us to analyze the system’s dynamics in a more convenient or meaningful way.

The equations will be replaced with the transformation equations.

$$\begin{aligned} \bar{r}_{T11} &= \begin{pmatrix} \cos\theta & -\sin\theta \\ \sin\theta & \cos\theta \end{pmatrix} \cdot \begin{pmatrix} b \\ 0 \end{pmatrix} = \begin{pmatrix} b.\cos\theta \\ b.\sin\theta \end{pmatrix} \\ \bar{r}_{T12} &= \begin{pmatrix} \cos\theta & -\sin\theta \\ \sin\theta & \cos\theta \end{pmatrix} \cdot \begin{pmatrix} a \\ 0 \end{pmatrix} = \begin{pmatrix} a.\cos\theta \\ a.\sin\theta \end{pmatrix} \end{aligned} \tag{17}$$

By substituting the transformation equations into the equations of motion, the displacement variables can be eliminated and represented in terms of angular displacements.

$$\begin{aligned} \bar{F}_{T11} &= \bar{F}_{K3} \\ \bar{F}_{T12} &= \bar{F}_{K4} \end{aligned} \tag{18}$$

After plugging in the translational branch transformation Equations (17) and (18) into Equation (19), it is possible to remove the rigid arm forces. Once the substitution is performed, the equations will be expressed in terms of tree across variables, cotree through variables, and cotree across variables.

This will make it easier to work with the equations and understand the relationships between the variables.

$$\begin{aligned} I.\bar{\alpha} - \bar{r}_{T11} \times \bar{F}_{T11} - \bar{r}_{T12} \times \bar{F}_{T12} &= \bar{0} \\ -I.\bar{\alpha} - \begin{pmatrix} a.\cos\theta \\ a.\sin\theta \end{pmatrix} \times \begin{pmatrix} 0 \\ -\bar{F}_1 \end{pmatrix} - \begin{pmatrix} b.\cos\theta \\ b.\sin\theta \end{pmatrix} \times \begin{pmatrix} 0 \\ \bar{F}_2 \end{pmatrix} & \end{aligned} \tag{19}$$

By substituting the terminal equations, we can obtain the following equations. We can simplify this equation even further, as shown below:

$$\begin{aligned} -I.\bar{\alpha} + a.\bar{F}_1.\cos\theta - b.\bar{F}_2.\cos\theta &= 0 \\ I\ddot{\theta} &= a.\bar{F}_1 - b.\bar{F}_2 \end{aligned} \tag{20}$$

with  $\bar{\alpha} = \ddot{\theta}$ .

• **Translational circuit equations**

Translational circuit equations are mathematical expressions used to analyze the dynamics of mechanical systems involving translational motion. We employed these equations to describe the relationships between forces, velocities, and displacements within the system.

Equation (21) representing the translational circuit can be evaluated directly from the graphs [18].

$$\begin{aligned} -\bar{r}_{M1} + \bar{r}_{M2} + \bar{r}_{K4} - \bar{r}_{K3} - \bar{r}_{T11} - \bar{r}_{T12} &= \bar{0} \\ \bar{r}_{K4} &= \bar{r}_{K3} = \bar{0} \end{aligned} \tag{21}$$

The equations for translational branch transformation can also be expressed using the system’s velocities or even accelerations.

$$\begin{aligned} -\dot{\bar{r}}_{M1} + \dot{\bar{r}}_{M2} - \dot{\bar{r}}_{T11} - \dot{\bar{r}}_{T12} &= \bar{0} \\ -\bar{v}_{M1} + \bar{v}_{M2} - \bar{\omega}_{M3} \times R_{M3}.\bar{r}_{T110} - \bar{\omega}_{M3} \times R_{M3}.\bar{r}_{T120} &= \bar{0} \end{aligned} \tag{22}$$

Equation (22) represents the balance of linear velocities of points  $M_1$  and  $M_2$ , taking into account the rotational motion of the rigid body, and  $\bar{v}_{M1}$ ,  $\bar{v}_{M2}$  represent the linear velocities of points  $M_1$  and  $M_2$ , respectively.

$$\begin{aligned} -\ddot{\bar{r}}_{M1} + \ddot{\bar{r}}_{M2} - \ddot{\bar{r}}_{T11} - \ddot{\bar{r}}_{T12} &= \bar{0} \\ -\bar{a}_{M1} + \bar{a}_{M2} - \bar{a}_{T11} - \bar{a}_{T12} &= \bar{0} \\ -\ddot{\bar{r}}_{M1} + \ddot{\bar{r}}_{M2} - \bar{\omega}_{M3} \times R_{M3}.\bar{r}_{T110} + (\bar{\omega}_{M3})^2.\bar{r}_{T11} - \bar{\omega}_{M3} \times R_{M3}.\bar{r}_{T120} & \\ + (\bar{\omega}_{M3})^2.\bar{r}_{T11} &= 0 \end{aligned} \tag{23}$$

Equation (23) represents the total acceleration of points  $M_1$  and  $M_2$  on the rigid body, taking into account the rotational motion of the body and the positions of points  $T_{11}$  and  $T_{12}$  relative to the body.

$$\begin{aligned} -\ddot{\vec{r}}_{M1} + \ddot{\vec{r}}_{M2} - \ddot{\vec{r}}_{T11} - \ddot{\vec{r}}_{T12} &= \vec{0} \\ -\bar{a}_{M1} + \bar{a}_{M2} - \bar{a}_{T11} - \bar{a}_{T12} &= \vec{0} \end{aligned} \tag{24}$$

$\bar{a}_{M1}$  and  $\bar{a}_{M2}$  represent the linear accelerations of points  $M_1$  and  $M_2$ , respectively.

$$-\ddot{\vec{r}}_{M1} + \ddot{\vec{r}}_{M2} - \bar{\omega}_{M3} \times R_{M3} \cdot \vec{r}_{T110} + (\bar{\omega}_{M3})^2 \cdot \vec{r}_{T11} - \bar{\omega}_{M3} \times R_{M3} \cdot \vec{r}_{T120} + (\bar{\omega}_{M3})^2 \cdot \vec{r}_{T11} = \vec{0} \tag{25}$$

These equations capture the dynamic relationships between the translational branches of the system, providing insights into how changes in velocity or acceleration propagate through the system.

### 5.2. Formulation Procedure

The process of formulation is a systematic and iterative approach to problem solving that involves developing mathematical models, deriving equations, solving them, and validating the results. Figure 3 show the process of formulation of the circuit and cutset equation.

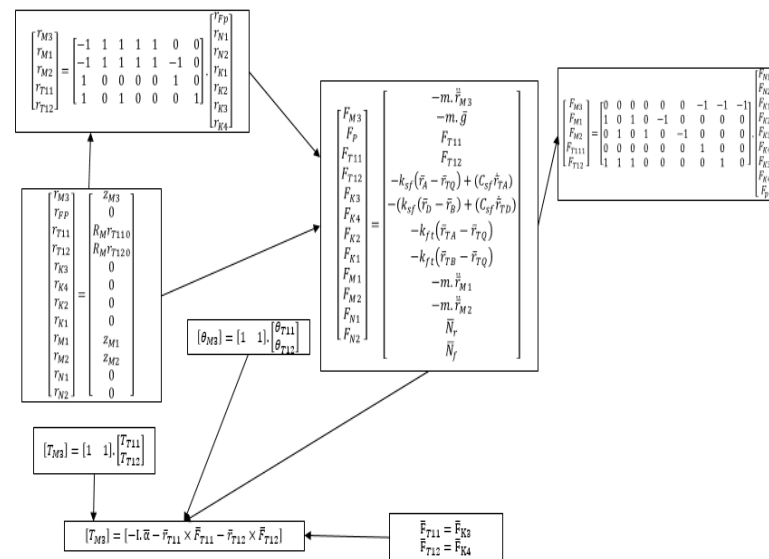


Figure 3. Formulation procedure.

In graph theory, topological equations describe the structural properties of graphs, while cutset equations are derived from the conservation of flow principle. These equations are useful in network flow analysis to determine maximum flows and minimum cuts.

#### - The circuit equation

It is important to know that while graph theory can help with understanding circuits, analyzing circuits usually requires a mix of algebraic equations, differential equations, and principles of physics. Even though there may be similarities between circuit components and graph elements, specialized techniques and equations are often needed for circuit analysis that go beyond just graph theory. Equation (26) shows the adjacency matrices of our system. These matrices illustrate the connections between nodes in the system, allowing us to understand the relationships and interactions among components and the system’s behavior.

$$\begin{bmatrix} r_{M3} \\ r_{M1} \\ r_{M2} \\ r_{T11} \\ r_{T12} \end{bmatrix} = \begin{bmatrix} -1 & 1 & 1 & 1 & 1 & 0 & 0 \\ -1 & 1 & 1 & 1 & 1 & -1 & 0 \\ 1 & 0 & 0 & 0 & 0 & 1 & 0 \\ 1 & 0 & 1 & 0 & 0 & 0 & 1 \end{bmatrix} \cdot \begin{bmatrix} r_{Fp} \\ r_{N1} \\ r_{N2} \\ r_{K1} \\ r_{K2} \\ r_{K3} \\ r_{K4} \end{bmatrix} \tag{26}$$

$$[\theta_{M3}] = [1 \quad 1] \cdot \begin{bmatrix} \theta_{T11} \\ \theta_{T12} \end{bmatrix} \tag{27}$$

- **The cutset equation**

When studying graph theory, a cutset refers to a set of edges that, once removed, will cause a graph to become disconnected into two or more components. Cutsets are crucial in analyzing the flow and connectivity of a graph. We used Equation (28) to determine the different properties associated with cuts in a graph.

$$\begin{bmatrix} F_{M3} \\ F_{M1} \\ F_{M2} \\ F_{T111} \\ F_{T12} \end{bmatrix} = \begin{bmatrix} 0 & 0 & 0 & 0 & 0 & 0 & -1 & -1 & -1 \\ 1 & 0 & 1 & 0 & -1 & 0 & 0 & 0 & 0 \\ 0 & 1 & 0 & 1 & 0 & -1 & 0 & 0 & 0 \\ 0 & 0 & 0 & 0 & 0 & 0 & 1 & 0 & 0 \\ 1 & 1 & 1 & 0 & 0 & 0 & 0 & 1 & 0 \end{bmatrix} \cdot \begin{bmatrix} F_{N1} \\ F_{N2} \\ F_{K1} \\ F_{K2} \\ F_{K3} \\ F_{K4} \\ F_{K3} \\ F_{K4} \\ F_p \end{bmatrix} \tag{28}$$

$$[T_{M3}] = [1 \quad 1] \cdot \begin{bmatrix} T_{T11} \\ T_{T12} \end{bmatrix} \tag{29}$$

The idea of cutsets is also closely linked to network flow analysis, especially in the area of network reliability and connectivity.

To describe a balance or equilibrium condition, with various forces and torques contributing to it.

$$\begin{aligned} -I\ddot{\alpha} + a\bar{F}_1 \cos\theta - b\bar{F}_2 \cos\theta &= \bar{0} \\ I\ddot{\theta} &= a\bar{F}_1 - b\bar{F}_2 \\ \bar{\alpha} &= \ddot{\theta} \end{aligned} \tag{30}$$

The equations governing under various forces and constraints of a half model of a motorcycle model can be expressed by

$$\begin{aligned} -m\ddot{z}_s - m\bar{g} - (k_{sf}(\bar{r}_D - \bar{r}_B) + (C_{sf}\dot{\bar{r}}_{TD})) - (k_{sf}(\bar{r}_A - \bar{r}_{TQ}) + (C_{sf}\dot{\bar{r}}_{TA})) &= \bar{0} \\ -m\ddot{z}_{uf} + \bar{N}_f - k_{ft}(\bar{r}_{TB} - \bar{r}_{TQ}) + \bar{F}_{k4} &= \bar{0} \\ -m\ddot{z}_{ur} + \bar{N}_r - k_{ft}(\bar{r}_{TA} - \bar{r}_{TQ}) + \bar{F}_{k3} &= \bar{0} \end{aligned} \tag{31}$$

with

$$\begin{aligned} \bar{F}_{k3} &= k_{sf}(\bar{r}_{TA} - \bar{r}_{TQ}) + (C_{sf}\dot{\bar{r}}_{TA}) \\ \bar{F}_{k4} &= k_{sf}(\bar{r}_{TD} - \bar{r}_{TB}) + (C_{sf}\dot{\bar{r}}_{TD}) \end{aligned} \tag{32}$$

The equations can be reformulated as follows:

$$M(\ddot{u}) + c(\dot{u}) + k(u) = R \tag{33}$$

$u = [z_E \theta z_C z_D]$ , which describes a state or configuration of a system, with components representing different positional and rotational aspects.

And  $R = [0, 0, F_{k3}, k_{k4}]$  represents the external forces applied to a vehicle body system, with

$$M = \begin{pmatrix} M_s & 0 & 0 & 0 \\ 0 & I & 0 & 0 \\ 0 & 0 & M_{usf} & 0 \\ 0 & 0 & 0 & M_{usr} \end{pmatrix}$$

$$K = \begin{pmatrix} k_{fs} + k_{rs} & k_{fs}a - k_{rs}b & -k_{fs} & -k_{rs} \\ k_{fs}a - k_{rs}b & C_{sf}a^2 + C_{sr}b^2 & -k_{fs}a & -k_{fs}b \\ -k_{fs} & -k_{fs}a & k_{fs} + k_{ft} & 0 \\ -k_{rs} & k_{rs}b & 0 & k_{fs} + k_{rt} \end{pmatrix}$$

$$C = \begin{pmatrix} C_{sf} + C_{sr} & C_{sf}a - C_{sr}b & -C_{sf} & -C_{sr} \\ C_{sf}a - C_{sr}b & C_{sf}a^2 + C_{sr}b^2 & -C_{sf}a & -C_{sr}b \\ -C_{sf} & -C_{sf}a & -C_{sr} & 0 \\ -C_{sr} & -C_{sr}b & 0 & -C_{sr} \end{pmatrix}$$

### 6. Results

To evaluate the effectiveness of our method and the formulation rooted in graph theory, subsequent to generating the dynamic equations and kinematic variables encompassing pitch angle, and the displacement of both front and rear parts, including the sprung and unsprung masses, we utilized the MATLAB R2022 program to execute the kinematics and dynamics equations. This enabled us to demonstrate the motorcycle’s performance in a vertical configuration.

By analyzing the simulation results, it is possible to carry out a performance analysis of how the suspension linkage will behave and how design changes will affect the suspension dynamics.

The graph below shows the reported force of the motorcycle’s front and rear suspension.

Figure 4 shows how the forces typically acting on the rear and front parts of the motorcycle vary over a period of time.

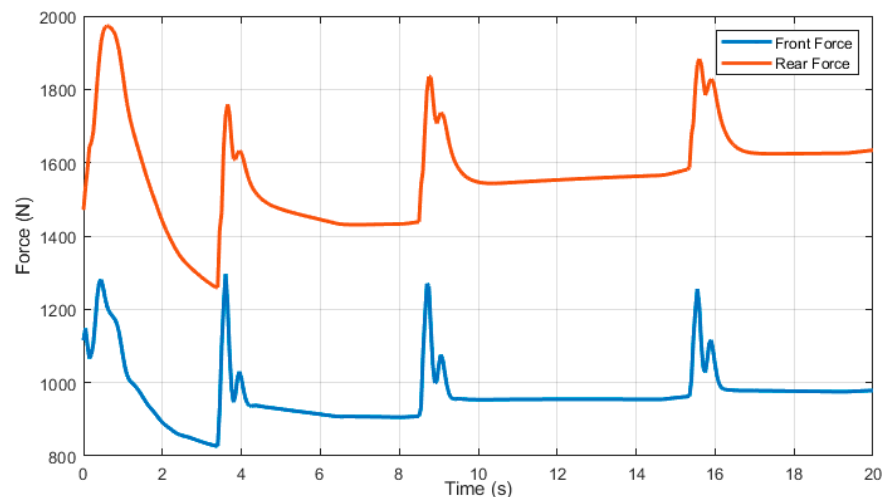
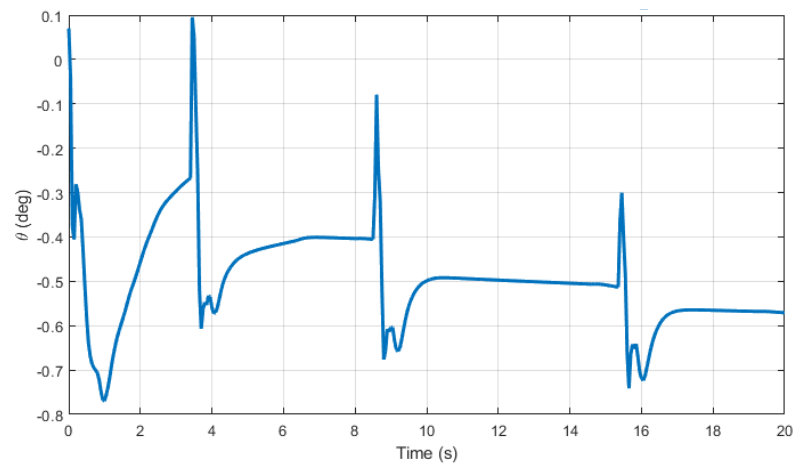


Figure 4. Force of rear and front part of motorcycle vs. time.

The maximum observed value on the front part of the motorcycle reached 1900 N, indicating a significant force exerted on the front end during the analyzed period. Conversely, the rear part of the motorcycle experienced a maximum force of 1300 N. This discrepancy in force magnitudes suggests a potentially notable difference in the distribution of forces between the front and rear parts of the motorcycle during the observed timeframe.

The graph below in Figure 5 shows the pitch angle of the main body. The pitch angle represents the tilt or inclination of the motorcycle’s body relative to the horizontal plane; it

provides valuable insights into the dynamic behavior of the motorcycle and helps identify areas for improvement in design, suspension tuning, and rider technique.



**Figure 5.** Pitch angle of motorcycle body vs. time.

The graph illustrates the reported pitch angle of the main body of the motorcycle. At its highest point, the pitch angle reaches  $0.75^\circ$ , indicating a significant tilt or inclination of the motorcycle's body relative to the horizontal plane during the analyzed period. This maximum pitch angle provides crucial information about the extent of the motorcycle's movement and its dynamic behavior.

The displacement represents the change in position of the rear and front parts of the motorcycle relative to their initial positions.

Figure 6 provides insight into the individual responses of both the front and rear parts of the motorcycle. Notably, the front suspension exhibits a maximum displacement of 21 mm, indicating the extent of its motion during the analyzed period. Conversely, the rear suspension experiences a compression of  $-10$  mm, suggesting a downward movement or compression of the suspension components. These observations highlight the dynamic behavior of both suspensions and contribute to understanding the overall performance and stability of the motorcycle under varying conditions.

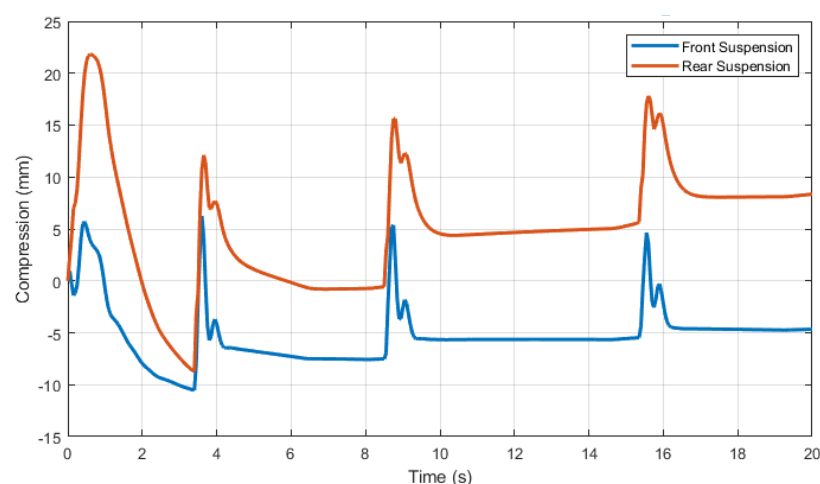


**Figure 6.** Displacement of rear and front part of motorcycle vs. time.

Table 4 provides a comparison between our model and other relevant studies, focusing on displacement and pitch angle, including Shahriar et al. [27], Pozuelo et al. [28], Dumitriu et al. [29], and our methodology. It shows the variations in displacement values for both the rear and front parts of the motorcycle, as well as differences in pitch angle readings.

Our model's accuracy in analyzing the vertical dynamics of motorcycles can be better understood by comparing it to previous work.

**Table 4.** Comparison of results.

Studies	Displacement of Rear Part of Motorcycle (mm)	Displacement of Front Part of Motorcycle (mm)	Pitch Angle (Degree)
Shahriar et al. [27]	15 mm	10 mm	0.45°
Our work	21 mm	10 mm	0.8°
Pozuelo et al. [28]	39 mm	39 mm	0.7°
Dumitriu et al. [29]	54 mm	46 mm	1.12°

Our study, along with Shahriar et al. [27], recorded lower displacements compared to Pozuelo et al. [28] and Dumitriu et al. [29]. Additionally, there is notable variation in the pitch angle among the studies, with Dumitriu et al. [29] having recorded the highest value. Our findings are more aligned with the pitch angle model proposed by Pozuelo et al. [28] compared to the notably higher value reported by Dumitriu et al. [29]. This finding contributes significantly to maintaining vehicle stability, a critical factor for safety, particularly when traveling at high speeds.

Table 4 also shows that our model performs comparably to the study conducted by Shahriar et al. [27], particularly in displacement prediction. These results highlight significant differences in the displacement of both the front and rear parts of motorcycles across various studies. As previous research has shown, the displacement of the rear part varies across the studies, with values ranging from 15 mm to 54 mm. In our work, the displacement falls in between these extremes at 21 mm, and our findings are more in line with the model suggested by Shahriar et al. [27] compared to the notably higher value reported by Dumitriu et al. [29] for the displacement of the front part.

The results of our study show a slight improvement compared to previous research. Our findings are consistent with the results of analytical work [27], experimental studies [28], and commercial software for 2D dynamics [29]. This is particularly evident in the examination of the pitch angle, the forces, and compression of both the front and rear part of the vertical model of a motorcycle.

## 7. Conclusions

The aim of this study was to introduce a novel formulation and mathematical model using graph theory principles to elucidate the core formulation. We have adopted graph theory as a new methodology to develop a new representation of the vertical dynamics of a motorcycle with four degrees of freedom, including suspension and tire models. We have enumerated the key steps necessary for generating the mathematical and dynamic equations. This methodical approach ensures clarity and accuracy in our formulation process and representation. Subsequently, we applied the dynamic equations to analyze the dynamic behavior of both the sprung and unsprung masses' vertical displacements, while considering the diverse conditions of the road profile. The simulation results were analyzed and summarized.

**Author Contributions:** Conceptualization, M.G. and A.S.; methodology, M.G., M.L.S. and A.S.; software, M.G.; validation, M.G., M.L.S. and H.M.; formal analysis, A.S. and H.M.; investigation, M.L.S.; resources, M.L.S.; data curation, H.M.; writing—original draft preparation, M.G. and M.L.S.; writing—review and editing, M.G. and M.L.S.; visualization, A.S. and H.M.; supervision, A.S.; project administration, M.L.S.; funding acquisition, M.G. and A.S. All authors have read and agreed to the published version of the manuscript.

**Funding:** This research received no external funding. The APC was funded by Transilvania University of Brasov.

**Data Availability Statement:** No new data were created or analyzed in this study.

**Acknowledgments:** We would like to express our gratitude to Catalin Iulian Pruncu for his valuable suggestion on how to better organize the paper and for his support.

**Conflicts of Interest:** The authors declare no conflicts of interest.

## Appendix A

**Table A1.** Numerical Values.

Parameter	Nomenclature	Value
Sprung mass	$m_s$	12,850 kg
Moment of inertia	$I$	3443.05 kgm <sup>2</sup>
Front unsprung mass	$m_{uf}$	1400 kg
Rear unsprung mass	$m_{ur}$	700 kg
Front wheelbase	$a$	1.716 m
rear wheelbase	$b$	1.271 m
Rear suspension stiffness	$K_3$	55,000 N/m
Front suspension stiffness	$K_4$	110,000 N/m
Front tire stiffness	$K_1$	116,000 N/m
Rear tire stiffness	$K_2$	232,000 N/m
Front suspension damping coefficient	$C_3$	640 Ns/m
Rear tire suspension coefficient	$C_4$	320 Ns/m

The matrix of transformation used in our system is

$$R^m(\theta) = \begin{pmatrix} \cos \theta & 0 & -\sin \theta \\ 0 & 1 & 0 \\ \sin \theta & 0 & \cos \theta \end{pmatrix}$$

The inertia tensor of the vehicle body is

$$I = \begin{pmatrix} 0 & 0 & 0 \\ 0 & 0 & 0 \\ 0 & 0 & I_{zz} \end{pmatrix}$$

## References

1. Gross, J.L.; Yellen, J. *Handbook of Graph Theory*; CRC Press: Boca Raton, FL, USA, 2003.
2. Morency, K. Automatic Generation of Real-Time Simulation Code for Vehicle Dynamics using Linear Graph Theory and Symbolic Computing. MASC Thesis, Department of Systems Design Engineering, University of Waterloo, Waterloo, ON, Canada, 2007.
3. Shi, P.; McPhee, J. Dynamics of flexible multibody systems using virtual work and linear graph theory. *Multibody Syst. Dyn.* **2000**, *4*, 355–381. [[CrossRef](#)]
4. Garziad, M.; Saka, A. An Overview of the Main Topics and Applications of Graph Theoretic Problems in Multiphysics Engineering. *J. Appl. Mech. Eng.* **2017**, *6*, 284. [[CrossRef](#)]
5. Bombardier, W.; McPhee, J.; Schmitke, C. Symbolic Formulation of Multibody Dynamic Equations for Wheeled Vehicle Systems on Three-Dimensional Roads. *SAE Int. J. Mater. Manuf.* **2010**, *3*, 454–467.
6. Schmitke, C.; Morency, K.; McPhee, J. Using graph theory and symbolic computing to generate efficient models for multi-body vehicle dynamics. *Proc. Inst. Mech. Eng. Part K J. Multi-Body Dyn.* **2008**, *222*, 339–352. [[CrossRef](#)]
7. Banerjee, J.M.; McPhee, J.J. Graph-Theoretic Modeling and Dynamic Simulation of an Automotive Torque Converter. In Proceedings of the 7th Vienna International Conference on Mathematical Modelling, Vienna, Austria, 14–17 February 2012; Troch, I., Ed.; Elsevier: Amsterdam, The Netherlands, 2012.
8. Amine, B. *Modélisation des Systèmes Multi-Corps Rigide Basée sur la Méthode des Réseaux Virtuels*; Université Laval: Quebec City, QC, Canada, 2010.
9. Schmitke, C.; McPhee, J. Using linear graph theory and the principle of orthogonality to model multibody, multi-domain systems. *Adv. Eng. Inform.* **2007**, *22*, 147–160. [[CrossRef](#)]
10. Al-Hakim, L.; Kusiak, A.; Mathew, J. A graph-theoretic approach to conceptual design with functional perspectives. *Comput.-Aided Des.* **2000**, *32*, 867–875. [[CrossRef](#)]

11. Vogt, H.S.; Schmitke, C.C.; Jalali, K.; McPhee, J.J. Unified modelling and real-time simulation of an electric vehicle. *Int. J. Veh. Auton. Syst.* **2008**, *6*, 288–307. [[CrossRef](#)]
12. Dunlop, J.; Khajepour, A. A new multi-terminal pulley model for use in graph theoretic modelling. *Mech. Mach. Theory* **2000**, *35*, 1601–1621. [[CrossRef](#)]
13. Sreeram, T.R. Graph theory based parametric influences applied to torsional vibration analysis. *Adv. Eng. Softw.* **2005**, *36*, 209–224. [[CrossRef](#)]
14. McPhee, J.; Redmond, S.M. Modelling multibody systems with indirect coordinates. *Comp. Methods Appl. Mech. Eng.* **2006**, *195*, 6942–6957. [[CrossRef](#)]
15. Dao, T.S.; McPhee, J. Dynamic modeling of electrochemical systems using linear graph theory. *J. Power Sources* **2011**, *196*, 10442–10454. [[CrossRef](#)]
16. Zawiślak, S.; Rysiński, J. (Eds.) . *Graph-Based Modelling in Engineering*; Springer International Publishing: Berlin/Heidelberg, Germany, 2017.
17. Cheng, D.; Liu, Y.; Qin, D.; Hu, M.; Wan, W.F. Analysis of the efficiency of the power coupling mechanism for tracked vehicle transmission based on the graph theory. In *Power Transmissions: Proceedings of the International Conference on Power Transmissions 2016 (ICPT 2016), Chongqing, China, 27–30 October 2016*; CRC Press: Boca Raton, FL, USA, 2017.
18. Chen, W.K. *Applied Graph Theory*; Elsevier: Amsterdam, The Netherlands, 2012; Volume 13.
19. Dörfler, F.; Simpson-Porco, J.W.; Bullo, F. Electrical networks and algebraic graph theory: Models, properties, and applications. *Proc. IEEE* **2018**, *106*, 977–1005. [[CrossRef](#)]
20. Huang, T.; Whitehouse, D.J. The use of graph theory to formulate the linear dynamic characteristics of rigid body systems. *Proc. R. Soc. Lond. Ser. A Math. Phys. Eng. Sci.* **1997**, *453*, 1299–1310. [[CrossRef](#)]
21. Lang, S.Y. Graph-theoretic modelling of epicyclic gear systems. *Mech. Mach. Theory* **2005**, *40*, 511–529. [[CrossRef](#)]
22. McPhee, J.J. A unified graph—Theoretic approach to formulating multibody dynamics equations in absolute or joint coordinates. *J. Frankl. Inst.* **1997**, *334*, 431–445. [[CrossRef](#)]
23. Hong, K.-T.; Lang, Y.T. A Graph Theoretic Approach to CAD for the Analysis of Planar Mechanisms, pdf-file. Available online: <https://citeseerx.ist.psu.edu/document?repid=rep1&type=pdf&doi=b27aa95c76ecc0d2e58db84a79deaf0e5828c919> (accessed on 27 April 2024).
24. Cossalter, V.; Lot, R.; Massaro, M. Motorcycle dynamics. In *Modelling, Simulation and Control of Two-Wheeled Vehicles*; John Wiley & Sons, Ltd.: Hoboken, NJ, USA, 2014; pp. 1–42.
25. McPhee, J.; Schmitke, C.; Redmond, S. Dynamic modelling of mechatronic multibody systems with symbolic computing and linear graph theory. *Math. Comput. Model.* **2004**, *10*, 1–23. [[CrossRef](#)]
26. McPhee, J.J. Automatic generation of motion equations for planar mechanical systems using the new set of “branch coordinates”. *Mech. Mach. Theory* **1998**, *33*, 805–823. [[CrossRef](#)]
27. Shahriar, A.; Rahman, K.A.; Tanvir, S. Simulation and analysis of half-car passive suspension system. *Mech. Eng. Res. J.* **2016**, *10*, 66–70.
28. Garcia-Pozuelo, D.; Gauchia, A.; Olmeda, E.; Diaz, V. Bump modeling and vehicle vertical dynamics prediction. *Adv. Mech. Eng.* **2014**, *6*, 736576. [[CrossRef](#)]
29. Melinte, O.D.; Dumitru, D.N. CARSIM software simulations of half-car vertical 2D dynamics and vehicle suspension behavior. In *The Annual Symposium of the Institute of Solid Mechanics SISOM*; Acta Technica Napocensis, Series: Applied Mathematics and Mechanics vol. 56, issue iv, November 2013. Available online: <https://docplayer.net/44987274-Carsim-software-simulations-of-half-car-vertical-2d-dynamics-and-vehicle-suspension-behavior.html> (accessed on 27 April 2024).

**Disclaimer/Publisher’s Note:** The statements, opinions and data contained in all publications are solely those of the individual author(s) and contributor(s) and not of MDPI and/or the editor(s). MDPI and/or the editor(s) disclaim responsibility for any injury to people or property resulting from any ideas, methods, instructions or products referred to in the content.